

Spectrophotometric Study of the Interaction Between Aza-15-Crown-5 and Some π -Acceptors in Chloroform Solution

Hamid Reza POURETEDAL¹, Abolfazl SEMNANI^{2*}
Mohammad Hossein KESHAVARZ¹ and Ali Reza FIROOZ²

¹Faculty of Science, Malek-ashtar University of Technology, Shahin-shahr-IRAN

²Faculty of Science, Shahrekord University, Shahrekord-IRAN
e-mail: a_semmeni@yahoo.com

Received 15.12.2004

A spectrophotometric study concerning the interaction between A15C5 as n-donor and TCNE, DDQ, TCNQ and bromanil as π -acceptor was been performed in chloroform at 25 °C. The results of TCNE indicate the formation of a 1:1 charge-transfer complex through a nonequilibrium reaction. In the case of DDQ, the formation of 1:2 (A15C5/DDQ) and 1:1 charge-transfer complexes through equilibrium and nonequilibrium reactions is confirmed. The formation constant of the equilibrium step was evaluated from the computer fitting of the absorbance-mole ratio data as $\log K_f = 5.14 \pm 0.09$. The $[A15C5^+(DDQ)_2^-]$ and $[A15C5^+DDQ^-]$ are suggested as the possible 1:2 and 1:1 adducts, respectively. The results of TCNQ are indicative of the gradual formation of two 1:1 equilibrium products. The $[A15C5^+TCNQ^-]$ and 7-A15C5-7,8,8-tricyanoquinodimethane are assigned to these adducts and the rate constant and sum of their formation constants are measured. In the case of bromanil, the conversion to a charge-transfer complex through a nonequilibrium reaction is observed. The rate constant of this reaction was determined. Finally, all of the resulting complexes were isolated in crystalline form and the effect of complex formation on IR spectra is discussed.

Key Words: Spectrophotometry, Azacrown ethers, TCNQ, DDQ, Bromanil, TCNE.

Introduction

Macrocyclic crown ethers, widely referred to as crown ethers, exhibit many interesting properties. The presence of cavities in these ethers, provided by the cyclic disposition of oxygen, confers unique ligational properties¹⁻⁵. During the past 2 decades interest has increased in the molecular complexes of crown ethers. Interest in this area is strongly stimulated by the possibility of applications in separation processes; preparation of ion-selective electrodes; conversion of chemical reactions into optical or electronic signals; the mimicking of enzymes in their capability to bind substances rapidly, selectively and reversibly; and

*Corresponding author

catalyzing of chemical reactions⁶. Thermodynamic and kinetic data for macrocycle interaction with neutral molecules were published by Izatt et al. in 1992⁶. Upon reviewing the work compiled in Izatt's review, only a few reports on the interaction of crown ethers with π -acceptors are observed⁷⁻⁹. The data are limited to benzocrown ethers⁷⁻⁹ and no information about nitrogen⁻ containing crown ethers is seen. Since then, several studies have been conducted by Shamsipur and co-workers¹⁰⁻¹². However, these reports are not efficient and the lack of data is felt clearly. In addition, there is an important need for one or more standard reactions to be studied in multiple laboratories. This has been done for metal-macrocycle interactions^{13,14} but not for molecule-macrocycle ones. Thus more research in this field is needed.

We are currently involved in the study of molecular complexes of crown ethers¹⁵⁻²². In this paper we report the results of our study on the interaction between A15C5 and π -acceptors, TCNE, DDQ, TCNQ and bromanil in chloroform solution.

Experimental

Aza-15-crown-5 (A15C5, Fluka) was recrystallized from reagent grade n-hexane and dried under vacuum over P₂O₅. The π -acceptors, from Merck, were used without any further purification except for vacuum drying over P₂O₅. The structures of azacrown ether and the π -acceptors are shown in Figure 1.

All UV-Vis spectra were recorded on a Perkin Elmer Lambda 2 spectrophotometer and the absorbance measurements were obtained with a Philips PU875 spectrophotometer at 25 ± 1 °C. Conductance measurements were carried out with a Metrohm 660 conductivity meter in a thermostated cell at 25 ± 1 °C.

In order to obtain UV-Vis spectra of the π -acceptors, upon the addition of A15C5, 3 mL of each π -acceptor solution was transferred to a 1-cm quartz cell and the spectra were recorded after direct addition of appropriate amounts of A15C5. A similar procedure was followed for monitoring the absorbance at fixed wavelength. In each case, additions were performed with a 100- μ L Hamilton syringe.

In order to prepare the charge-transfer complexes of π -acceptors with A15C5 in crystalline form, 5 mL solutions containing equimolar amounts of π -acceptors and A15C5 were prepared in chloroform. The resulting solutions were then filtered and transferred into crystallization dishes. The solution was allowed to evaporate for about 20 h. The resulting solid crystals were collected and dried under vacuum for 12 h. The dried crystals were used for obtaining IR spectra and melting point measurements. IR spectra were recorded on a Shimadzu IR-470 spectrophotometer using KBr pellets. A Gallenham apparatus measured the melting points.

Results and Discussion

A. TCNE: The absorption spectra of 8.33×10^{-3} M TCNE in the presence of varying concentrations of A15C5 are shown in Figure 2. As can be seen, in the presence of A15C5 a new band appears in the 350-450 nm region. None of the initial reactants show any measurable absorption in this region. Therefore, the observation of this band can be assigned to the formation of charge transfer complex between A15C5 and TCNE²³. A15C5 and TCNE in this complex behave as n-donor and π -acceptor, respectively²⁴. Since no isosbestic point is observed, a nonequilibrium pathway is followed²⁵.

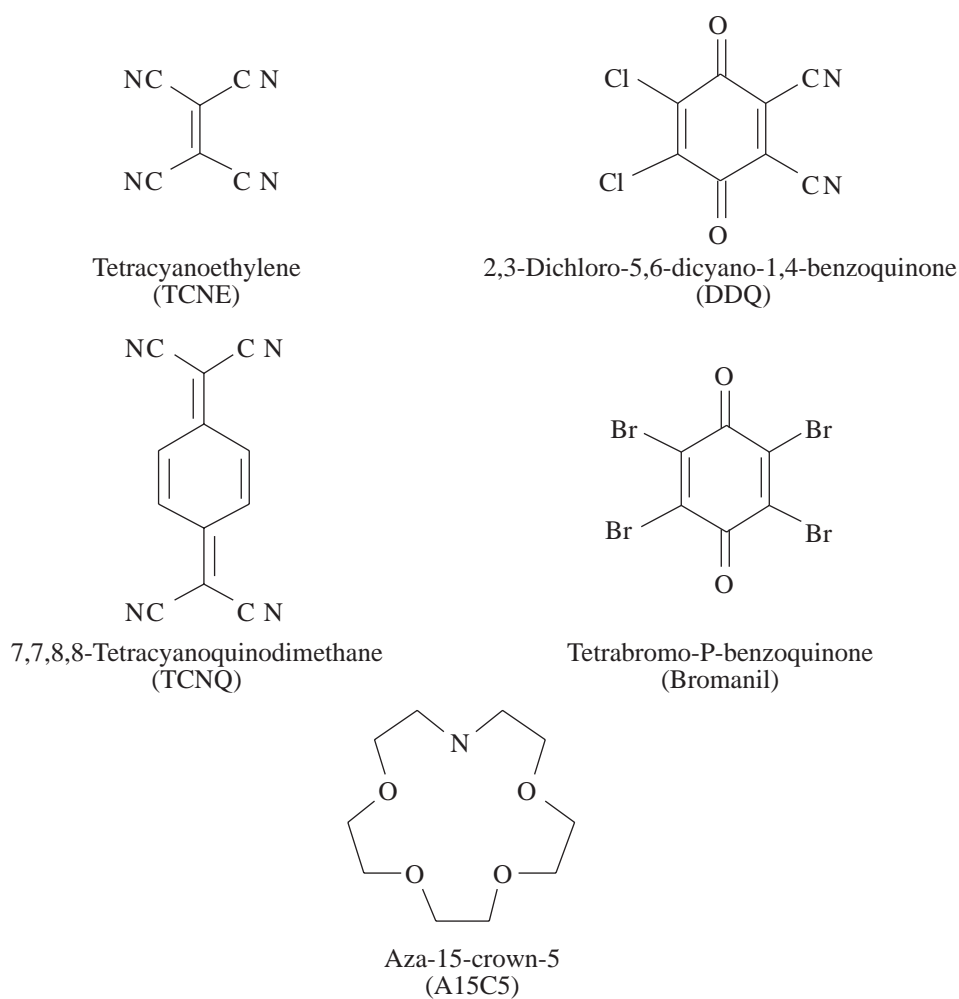


Figure 1. Structure of azacrown ether and π -acceptors.

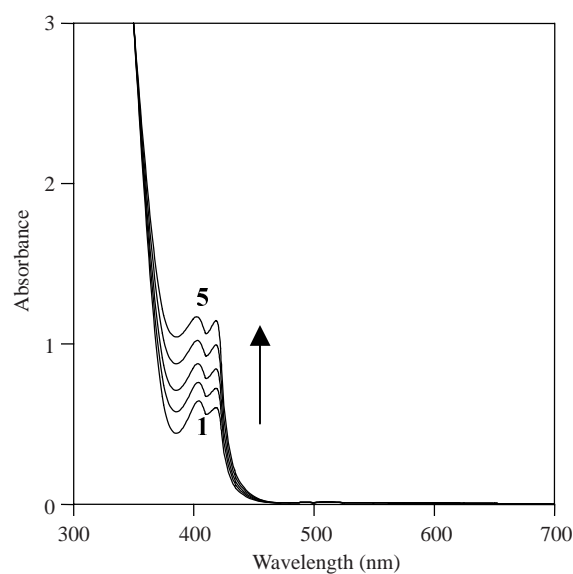


Figure 2. Absorption spectra of 8.33×10^{-3} M TCNE in the presence of varying concentrations of A15C5. The A15C5/TCNE mole ratios are: 1; 0.15, 2; 0.30, 3; 0.47, 4; 0.65 and 5, 0.94.

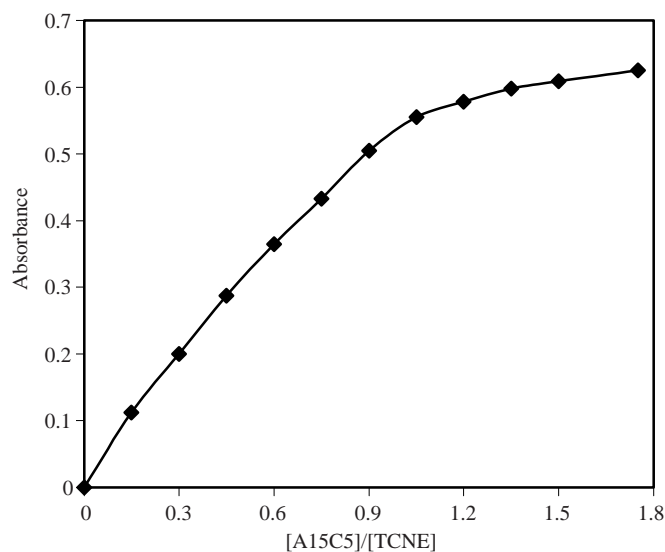


Figure 3. Plot of absorbance vs. A15C5/TCNE mole ratios in chloroform solution obtained at 432 nm.

In order to obtain the stoichiometry of the resulting complex, the absorbance-mole ratio method²⁶ was followed. The corresponding plot is shown in Figure 3. The plot clearly indicates the formation of a 1:1 complex.

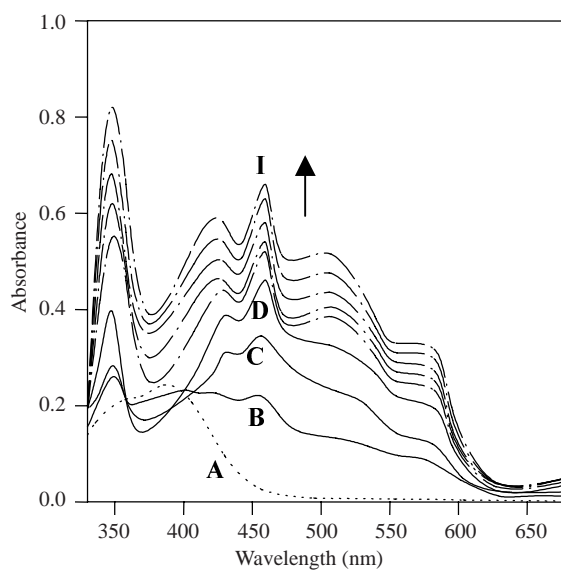


Figure 4. Absorption spectra of 3.17×10^{-4} M DDQ in the presence of varying concentrations of A15C5. The A15C5/DDQ mole ratios are: A; 0.0, B; 0.19, C; 0.37, D; 0.50, E; 0.754, F; 0.93, G; 1.12, H; 1.30, I; 1.50.

B. DDQ: Figure 4A shows the absorption spectrum of 3.17×10^{-4} M DDQ in the absence of A15C5. Figures 4B-4D show the absorption spectra of DDQ in the presence of 5.90×10^{-5} , 1.18×10^{-4} and 1.59×10^{-3} M A15C5 (the corresponding A15C5/DDQ mole ratios are 0.19, 0.37 and 0.50, respectively). The appearance of new bands in the 300-600 nm region, along with the observation of an isosbestic point at 358 nm, is indicative of an equilibrium charge transfer interaction between DDQ and A15C5²⁵.

It should be noted that at A15C5/DDQ mole ratios more than 0.5 (Figures 4E-4G), the isosbestic point is broken. This means that at mole ratios more than 0.5 a nonequilibrium reaction will follow.

According to the previous 2 paragraphs, the following equations are suggested for the interaction of A15C5 and DDQ at various A15C5/DDQ mole ratios.



These equations are confirmed by the frequent formation of DDQ radical anion with various donors²⁷⁻³⁰ and the formation of similar dimers of some other π -acceptors³¹.

Figure 5 shows the plots of absorbance vs. A15C5/DDQ mole ratio obtained at 500 and 350 nm. Both plots show a break at A15C5/DDQ = 0.5 and further confirm the suggested mechanism (Eqs. 1 and 2).

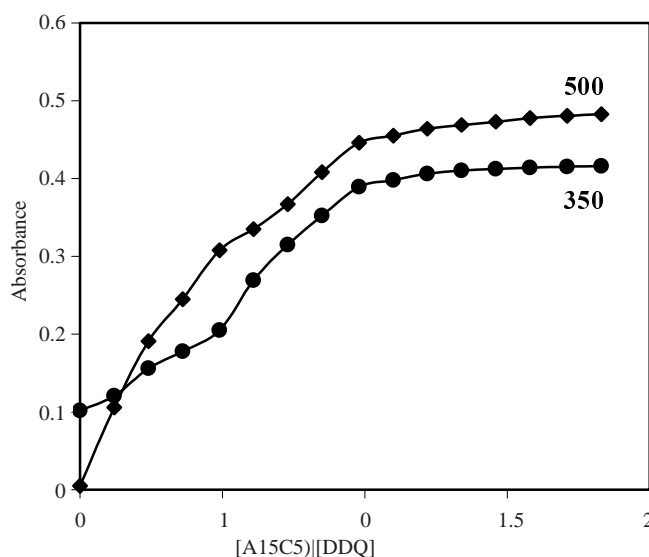


Figure 5. Plots of absorbance vs. A15C5/DDQ mole ratios in chloroform solution obtained at 500 and 350 nm.

For evaluation of the formation constants of the resulting 1:2 A15C5:DDQ complex (Eq. 1), K_f , from the absorbance-mole ratio data, the nonlinear least-squares curve fitting program KINFIT was used³². The program is based on the iterative adjustment of calculated to observed absorbance values by using either the Wentworth matrix technique³³ or the Powell procedure³⁴. Adjustable parameters are K_f and ε , where ε is the molar absorption coefficient of the complex.

Equation 3 gives the observed absorbance of the complex at 500 nm. The mass balance equations can be written as Eqs. 4 and 5, and the formation constant of the complex as in Eq. 6.

$$A_{obs} = \varepsilon[A15C5^+(DDQ)_2^-] \quad (3)$$

$$C_{DDQ} = [DDQ] + 2[A15C5^+(DDQ)_2^-] \quad (4)$$

$$C_{A15C5} = [A15C5] + [A15C5^+(DDQ)_2^-] \quad (5)$$

$$K_f = [A15C5^+(DDQ)_2^-]/[A15C5][DDQ]^2 \quad (6)$$

Substitution of Eqs. 4 and 5 into 6 and rearrangement yields Eq. 7.

$$(2K_f - 1)[A15C5^+(DDQ)_2^-]^2 - K_f(C_{DDQ} + 2C_{A15C5})[A15C5^+(DDQ)_2^-] + K_f C_{DDQ} C_{A15C5} = 0 \quad (7)$$

The complex concentrations, $[A15C5^+(DDQ)_2^-]$, were calculated from Eq. 7 by means of a Newton-Raphson procedure. Once the value of $[A15C5^+(DDQ)_2^-]$ had been obtained, the concentrations of all other species involved were calculated from the corresponding mass balance equations by using the estimated value of K_f at the current iteration step of the program. Refinement of the parameters was continued until the sum-of-squares of the residuals between calculated and observed absorbance values for all experimental points was minimized. The output of the program KINFIT comprises the refined parameters, the sum of squares and the standard deviation of the data. Figure 6 shows the resulting computer fit of the absorbance mole ratio data. The data are due to A15C5/DDQ mole ratios in the range of 0-0.5. As seen, the fair agreement between the calculated and observed absorbances further supports the existence of a 1:2 complexation between A15C5 and DDQ in chloroform solution. The $\log K_f$ value obtained by this procedure is 5.14 ± 0.09 .

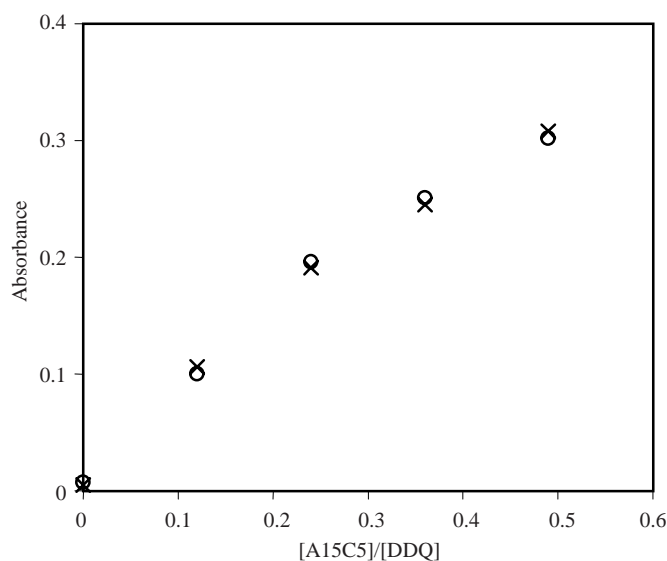


Figure 6. Computer fit of absorbance vs. A15C5/DDQ mole ratios 500 nm, (x) experimental and (O) calculated points.

C. TCNQ: Figure 7A shows the absorption spectrum of 2.61×10^{-3} M TCNQ in the absence of A15C5. The other spectra have been recorded in the presence of a 4.85×10^{-3} M A15C5 and in time periods of 5 min. As can be seen, over time the intensity of TCNQ band decreases gradually and simultaneously 2 new bands appear in the 300-375 nm and 450-650 nm regions. The existence of 2 isosbestic points at 340 nm and 440 nm is also detected. Such observations are indicative of the formation of 2 different charge transfer complexes through an equilibrium reaction³⁵.

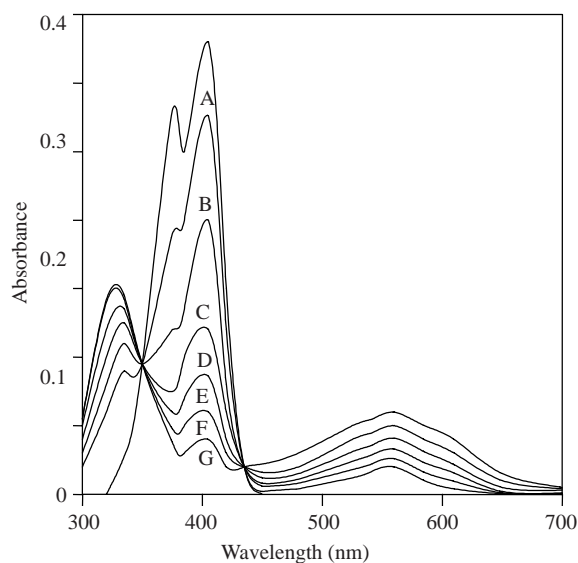
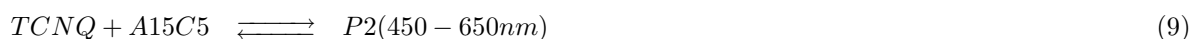


Figure 7. Absorption spectra of 2.61×10^{-3} M TCNQ (A) and 2.61×10^{-3} M TCNQ in the presence of 4.85×10^{-3} M A15C5 in time intervals of 5 min (B-G).



The reaction of TCNQ with the cyclic secondary amine pyrrolidine (Figure 8A) gives a product³⁵. The resulting adduct is assigned the structure 7-pyrrolidino-7,8,8-tricyanoquinodimethane (Figure 8B) on the basis of a spectroscopic investigation and elemental analysis³⁶. On the other hand, the formation of TCNQ^- radical anions has been recorded frequently³⁷⁻³⁹. Based on these observations it can be concluded that the 2 new bands are due to TCNQ^- radical anion (300-375 nm) and 7-A15C5-7,8,8- tricyanoquinodimethane (Figure 8C, 450-650 nm region). The similar behavior of some other azacrown ethers supports this idea¹⁵.

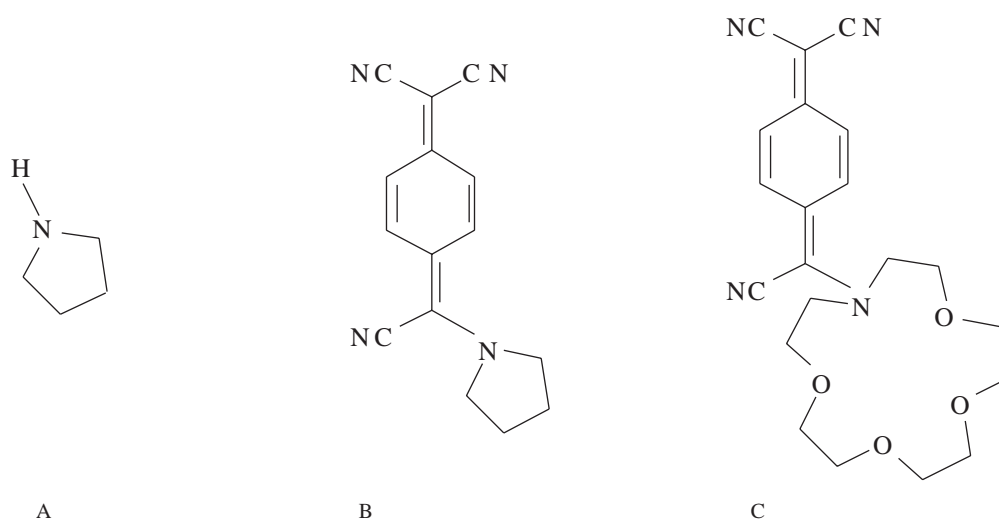


Figure 8. The structures of pyrrolidine (A), 7-pyrrolidino-7,8,8-tricyanoquinodimethane (B) and 7-A15C5-7,8,8-tricyanoquinodimethane (C).

The kinetics of the conversion of TCNQ to the corresponding products were followed by monitoring the absorbance as a function of time at 400 nm. The absorbance changes were found to be in accord with first order kinetics. The rate constant obtained from the slope of the $\text{Ln } A_t/A_o$ vs. t (Figure 9) is $k = 0.08 \text{ min}^{-1}$.

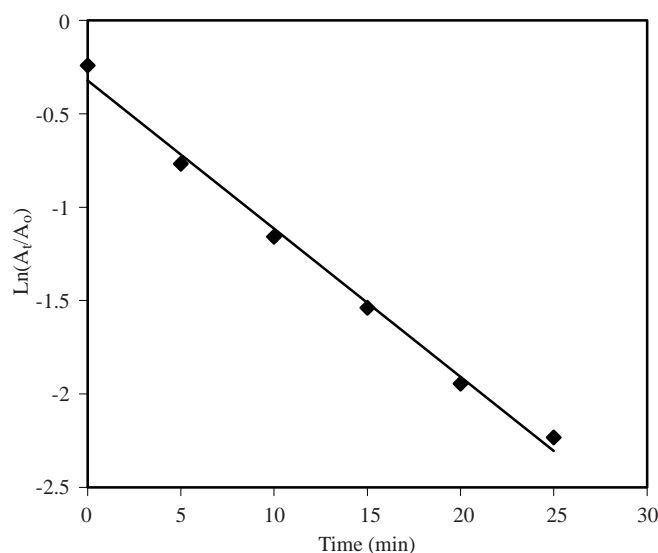


Figure 9. Plot of $\text{Ln}(A_t/A_o)$ vs. time at 400 nm for $2.61 \times 10^{-3} \text{ M}$ TCNQ and $4.85 \times 10^{-3} \text{ M}$ A15C5 mixture.

The formation constants of TCNQ complexation can be written as follows:

$$K1 = [P1]/[TCNQ][A15C5] \quad (10)$$

$$K2 = [P2]/[TCNQ][A15C5] \quad (11)$$

The sum of the above equations is equal to:

$$K1 + K2 = ([P1] + [P2])/[TCNQ][A15C5] \quad (12)$$

The mass balance equations for TCNQ and A15C5 are:

$$[TCNQ]_o = [TCNQ] + [P1] + [P2] \quad (13)$$

$$[A15C5]_o = [A15C5] + [P1] + [P2] \quad (14)$$

The concentration of TCNQ at each time can be determined by following the corresponding absorbance at 400 nm.

$$[TCNQ] = [TCNQ]_o(A/A_o) \quad (15)$$

where A and A_o are the absorbance of solution at 400 nm at each time and at the start of the of reaction, respectively. According to Eqs. 13 and 14, if the initial concentrations of A15C5 and TCNQ are the same, the concentrations at each time will also be equal. Under these conditions, the substitution of Eqs. 13, 14 and 15 in Eq. 12 yields:

$$K1 + K2 = (1 - (A/A_o r))/[TCNQ]_o(A/A_o)^2 \quad (16)$$

By measurement of absorbances at various time intervals, the value of $\log(K_1+K_2)=4.19 \pm 0.11$ was obtained. This value indicates that K_1 , K_2 or both are high, confirmed by the relative increasing of bands due to P1 and P2 adducts.

D. Bromanil: The absorption spectrum of 1.26×10^{-3} M bromanil is shown in Figure 10A. Figures 10B-10G are the spectra of bromanil in the presence of 4.55×10^{-3} M A15C5, which have been recorded at 5 min intervals. The appearance of a new band in the 450-650 nm region is indicative of the formation of a charge transfer product²³. The absence of an isobestic point indicates that the product is formed through a nonequilibrium reaction²⁵.

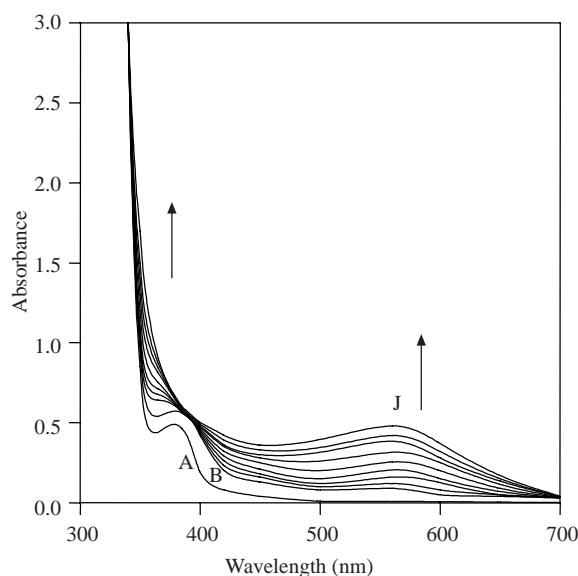


Figure 10. Absorption spectra of 1.26×10^{-3} M bromanil (A) and 1.26×10^{-3} M TBrBQ in the presence of 4.55×10^{-3} M A15C5 in time intervals of 5 min (B-J).

On the other hand, besides the formation of a charge transfer absorption band, an increase in the intensity of the bromanil band at 400 nm and a blue shift are also observed (Figure 10). This may be a direct result of the partial transfer of an electron to an antibonding orbital in the acceptor, which would increase the effective size of the acceptor so that the excitation energy is increased⁴⁰. The increasing effective size will result in a higher intensity absorption cross section being observed⁴¹.

The rate constant of the formation of the charge transfer product between A15C5 and bromanil was calculated by the Guggenheim method⁴² using the relationship $\ln(A_\infty - A_t) = -k(t - t_0) - \ln(A_\infty - A_0)$, where A_t and A_∞ are the absorbances of the 515 nm band at time t and infinite time, respectively. The rate constant obtained from the corresponding plot (Figure 11) is 0.04 min^{-1} .

E. IR spectra: The melting points and the IR spectral data of all π -acceptors, the 1:1 charge transfer complexes and A15C5 are presented in Table 1. As can be seen, the CN stretching of TCNE and CO stretching of DDQ show a drastic shift to lower and higher frequencies, respectively, upon molecular complex formation with A15C5. These shifts are indicative of a higher charge density on the cyano and a lower charge density on the carbonyl groups of the π -acceptors TCNE and DDQ charge transfer complexes, respectively. However, the methylene stretching of the ethoxy groups of A15C5 observed in the 2980-2810

cm^{-1} region did not show any considerable shift upon complex formation. This is probably due to the negligible contribution of the ethoxy groups in the interaction with π -acceptors⁴³.

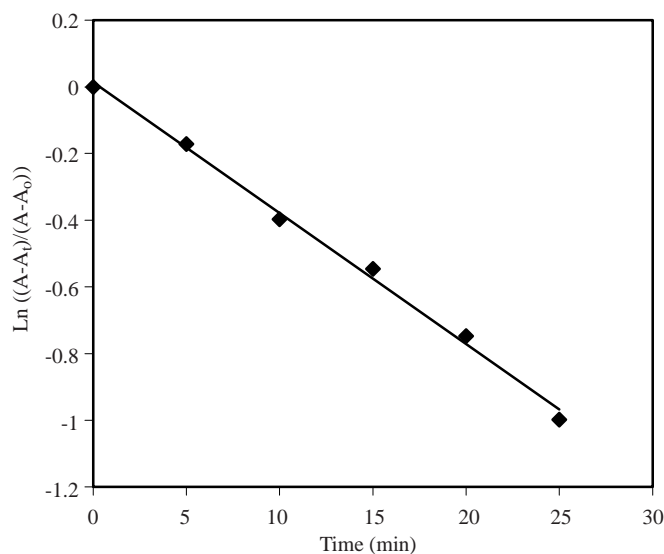


Figure 11. Plot of $\text{Ln}((A_{\infty}-A_t)/(A_{\infty}-A_o))$ vs. t at 550 nm for a 1.26×10^{-3} M bromanil and 4.55×10^{-3} M A15C5 mixture.

Table 1. Melting points and IR spectral data of π -acceptors, A15C5 and charge transfer adducts.

Compound	Melting point ($^{\circ}\text{C}$)	Wavenumber (cm^{-1})		
		CN	CO	NH
TCNE	197	2228	-	-
DDQ	213	2236	1675	-
TCNQ	288	2200	-	-
Bromanil	297	-	1673	-
A15C5	37.5	-	-	3350
TCNE-A15C5	53	2119	-	3365
DDQ-A15C5	384	2230	1710	3371
TCNQ-A15C5	309	2210, 2228, 2241	-	3389
Bromanil-A15C5	81	-	1683	3357

It is interesting to note that upon complexation of TCNQ, in the CN stretching region 3 bands are observed. These bands can be attributed to the CN of TCNQ radical anion (2210 cm^{-1}) and 2 kinds of CN in 7-A15C5-7,8,8-tricyanoquinodimethane (Figure 8C).

On the other hand, the NH stretching band of A15C5 shifted to higher frequencies in all complexes. This is reasonable based on the increasing polarity of the NH band during complexation.

Similar to DDQ, the CO stretching band of bromanil shifted to higher frequencies. However, the shift is much less than that of DDQ, which indicates a weaker interaction of A15C5-bromanil than of A15C5-DDQ.

Finally, a comparison of the melting points is indicative of a large increase in melting point for A15C5-DDQ and A15C5-TCNQ relative to the others, which is a result of the formation of ionic crystals in DDQ and TCNQ complexes.

F. Conductivity measurements: The conductance of various π -acceptors in the presence of A15C5 was measured for all cases but only small increases were observed. The small increase in conductance during

complexation shows that the charge transfer complexes are mainly ion pair and there is a little free ion in solution.

Conclusion

1. The complexes of all the π -acceptors studied show a charge transfer absorption band.
2. All of the complexes are mostly in the form of an ion pair.
3. TCNE and bromanil have nonequilibrium reactions, while DDQ and TCNQ have equilibrium reactions.
4. Because of the higher curvature of the absorbance-mole ratio of TCNE (Figure 3), relative to DDQ (Figure 5), complexes of the former are stronger than those of the latter.
5. The interaction of TCNQ and A15C5 causes the formation of 2 stable adducts.
6. Among the π -acceptors studied bromanil forms the weakest complex and only partial charge transfer from donor to acceptor occurs. This can be attributed to the lower electron withdrawing strength of bromanil relative to substituents in TCNE, DDQ and TCNQ.
7. The significant changes in NH IR bands indicate that in all cases the donation is due to nitrogen and the oxygen atoms of A15C5 do not take part in complexation.
8. The melting points are indicative of the formation of ionic crystals by DDQ and TCNQ and nonionic crystals by TCNE and bromanil.

References

1. C.J. Pedersen, **J. Am. Chem. Soc.** **89**, 2945 (1967).
2. D.J. Cram and J.M. Cram, **Acc. Chem. Res.** **11**, 8 (1978).
3. K. Morakum, **Acc. Chem. Res.** **10**, 294 (1977).
4. A. Semnani and M. Shamsipur, **J. Chem. Soc., Dalton Trans.** 2215 (1996).
5. A. Semnani and M. Shamsipur, **Spectrochim Acta** **49**, 411 (1993).
6. R.M. Izatt, J.S. Bradshaw, K. Pawlak, R.L. Bruening and B.J. Tarbet, **Chem. Rev.** **92**, 1261 (1992).
7. R. Mallini and V. Krishnan, **J. Phys. Chem.** **84**, 551 (1980).
8. R. Mallini and V. Krishnan, **Spectrochim. Acta** **40A**, 323 (1984).
9. Y. Jayathirtha and V. Krishnan, **Natl. Acad. Sci. Lett. (India)**, **1**, 365 (1978).
10. J. Zolgharnein and M. Shamsipur, **Polish J. Chem.** **72**, 2486 (1998).
11. S. Sadeghi, N. Alizadeh and M. Shamsipur, **J. Incl. Phenom.** **34**, 431 (1999).
12. M. Shamsipur, Z. Talebpour and N. Alizadeh, **J. Solution Chem.** **32**, 227 (2003).
13. R.M. Izatt, J.S. Bradshaw, S.A. Nielson, J.J. Lamb, J.S. Christensen and D. Sen, **Chem. Rev.** **85**, 271 (1985).
14. R.M. Izatt, K. Pawlak, J.S. Bradshaw and R.L. Bruening, **Chem. Rev.** **91**, 1721 (1991).
15. H.R. Pouretedal, A. Semnani, B. Nazari and A. Firooz, **Asian J. of Chem.** **17**, 329 (2005).
16. H.R. Pouretedal, A. Semnani, B. Nazari and A. Firooz, **Asian J. of Chem.** **17**, 2159 (2005).

17. A. Semnani, B. Shareghi and M.R. Sovizi, **Iranian J. of Chem. & Chem. Eng.** **19**, 67 (2000).
18. A. Semnani, H.R. Pouretdal and B. Shareghi, **Iranian J. of Chem. & Chem. Eng.** **23**, 1 (2004).
19. A. Semnani, H.R. Pouretdal, B. Nazari and A. Firooz, **Iranian J. of Chem. & Chem. Eng.** **23**, 27 (2004).
20. A. Semnani, H.R. Pouretdal, B. Nazari and A. Firooz, **Scientia Iranica** **10**, 1 (2003).
21. M. Shamsipur and H.R. Pouretdal, **J. Chin. Chem. Soc.** **51**, 1 (2004).
22. A. Semnani and M. Shamsipur, **J. Incl. Phenom.** **22**, 99 (1995).
23. L.J. Andrews and R.M. Keefer, "Molecular Complexes in Organic Chemistry", Holden Day, New York (1964).
24. M.T. Beck and I. Nagypal, "Chemistry of Complex Equilibria", John Wiley & Sons (1990).
25. D.A. Skoog, D.W. West and J. Holler, "Fundamental of Analytical Chemistry", Saunders College Publishing (1998).
26. J.B. Arteburn, **Tetrahedron** **57**, 9765 (2001).
27. T. Satoh, A. Nakamura and A. Iriuchijm, **Tetrahedron**, **57**, 9689 (2001).
28. G. Bringmann and S. Tasler, **Tetrahedron** **57**, 31 (2001).
29. S. Ma, X.D. Zhang and L.L. Shen, **J. of Photochem. Photobiol.** **139**, 97 (2001).
30. R. Foster, "Organic Charge-Transfer Complexes", Academic Press, London and New York (1969).
31. G.D. Christian and J.E. O'Reilly, "Instrumental Analysis", Allyn and Bacon (1986).
32. V.A. Nicely and J.L. Dye, **J. Chem. Educ.** **48**, 443 (1971).
33. W.E. Wentworth, **J. Chem. Educ.** **42**, 162 (1962).
34. M.J.D. Powell, **Comput. J.** **7**, 155 (1964).
35. W.R. Hertler, H.D. Hartzler, D.S. Acker and R.L. Benson, **J. Am. Chem. Soc.** **84**, 3387 (1962).
36. M.C. Gossel and S.C. Weston, **J. Phys. Org. Chem.** **5**, 533 (1992).
37. L.R. Melby, R.J. Harder, W.R. Hertler, R.L. Benson and W.E. Mochel, **J. Am. Chem. Soc.** **84**, 3374 (1962).
38. A.F. Garito and A.J. Heeger, **J. Acc. Chem. Res.** **7**, 232 (1974).
39. R.C. Wheland and J.L. Gillson, **J. Am. Chem. Soc.** **98**, 3916 (1976).
40. N.S. Bhacca and D.H. Williams, **Tetrahedron Lett.** 3127 (1964).
41. I.N. Levine, "Molecular Spectroscopy", Wiley-Interscience, (1975).
42. H.A. Benesi and J.H. Hildebrand, **J. Am. Chem. Soc.** **71**, 2703 (1949).
43. A.M. Nour El-Din, **Spectrochim. Acta** **42A**, 631 (1986).